AFRL-RW-EG-TP-2008-7405

MOISTURE EFFECTS ON THE HIGH STRAIN-RATE BEHAVIOR OF SAND (PREPRINT)

Bradley E. Martin (AFRL/RWMW)
Damage Mechanisms Branch
Air Force Research Laboratory
Munitions Directorate
Eglin AFB, FL 32542

Stephen A. Akers
U.S. Army Engineering Research
& Development Center (USAERDC)
3909 Halls Ferry Road
Vicksburg, MS 39180

Weinong Chen
Bo Song
Department of Aeronautics
and Astronautics Engineering
Purdue University
West Lafayette, IN 47907

APRIL 2008

JOURNAL ARTICLE (PREPRINT)

This paper was submitted for publication to the Mechanics of Materials Journal and if published will appear in the special edition, Advances in Granular Materials. One or more of the authors is a U.S. Government employee working within the scope of their position. Should any party assert copyrights, the U.S. Government, as joint owner of the work, has for itself and others acting on its behalf, the right to copy, distribute, and use the work by or on behalf of the U.S. Government.

This work has been submitted for publication in interest of the scientific and technical exchange. Publication of this report does not constitute approval or disapproval of the ideas or findings.

DISTRIBUTION A: Approved for public release; distribution unlimited.
96TH ABW/PA Public Release Confirmation #02-06-08-055;
dated 6 February 2008.

AIR FORCE RESEARCH LABORATORY, MUNITIONS DIRECTORATE

■ **Air Force Material Command** ■ **United States Air Force** ■ **Eglin Air Force Base**

REPORT DOCUMENTATION PAGE

Form Approved
OMB No. 0704-0188

The public reporting burden for this collection of information is estimated to average 1 hour per response, including the time for reviewing instructions, searching existing data sources, gathering and maintaining the data needed, and completing and reviewing the collection of information. Send comments regarding this burden estimate or any other aspect of this collection of information, including suggestions for reducing the burden, to Department of Defense, Washington Headquarters Services, Directorate for Information Operations and Reports (0704-0188), 1215 Jefferson Davis Highway, Suite 1204, Arlington, VA 22202-4302. Respondents should be aware that notwithstanding any other provision of law, no person shall be subject to any penalty for failing to comply with a collection of information if it does not display a currently valid OMB control number.

PLEASE DO NOT RETURN YOUR FORM TO THE ABOVE ADDRESS.

1. REPORT DATE *(DD-MM-YYYY)*	2. REPORT TYPE	3. DATES COVERED *(From - To)*
XX-04-2008	JOURNAL ARTICLE (PREPRINT)	

4. TITLE AND SUBTITLE

MOISTURE EFFECTS ON THE HIGH STRAIN-RATE BEHAVIOR OF SAND (PREPRINT)

5a. CONTRACT NUMBER

N/A

5b. GRANT NUMBER

N/A

5c. PROGRAM ELEMENT NUMBER

62602F

6. AUTHOR(S)

1. Bradley E. Martin
2. Weinong Chen
3. Stephen A. Akers
4. Bo Song

5d. PROJECT NUMBER

2502

5e. TASK NUMBER

12

5f. WORK UNIT NUMBER

29

7. PERFORMING ORGANIZATION NAME(S) AND ADDRESS(ES)

1. Air Force Research Laboratory
Munitions Directorate
AFRL/RWMW
Eglin AFB, FL 32542-6810

2. Department of Aeronautics
and Astronautics Engineering
Purdue University
West Lafayett, IN 47907

3. U.S. Army Engineering Research
& Development Center (USAERDC)
3909 Halls Ferry Road
Vicksburg, MS 39180

8. PERFORMING ORGANIZATION REPORT NUMBER

AFRL-RW-EG-TP-2008-7405

9. SPONSORING/MONITORING AGENCY NAME(S) AND ADDRESS(ES)

Air Force Research Laboratory
Munitions Directorate
AFRL/RWMW
Eglin AFB, FL 32542-6810

10. SPONSOR/MONITOR'S ACRONYM(S)

AFRL-RW-EG

11. SPONSOR/MONITOR'S REPORT NUMBER(S)

SAME AS BLOCK 8

12. DISTRIBUTION/AVAILABILITY STATEMENT

DISTRIBUTION A: Approved for public release; distribution unlimited.
96TH ABW/PA Public Release Confirmation #02-06-08-055;
dated 6 February 2008.

13. SUPPLEMENTARY NOTES

See 'cover page' for pertinent metadata information.

14. ABSTRACT

The effects of moisture content on the high strain rate mechanical properties of fine grain sand were characterized with a split-Hopkinson pressure bar.

See journal article for complete abstract.

15. SUBJECT TERMS

Dynamic, Hopkinson bar, pulse shaping, moisture content, sand, high strain-rate

16. SECURITY CLASSIFICATION OF:			17. LIMITATION OF ABSTRACT	18. NUMBER OF PAGES	19a. NAME OF RESPONSIBLE PERSON
a. REPORT	b. ABSTRACT	c. THIS PAGE			Bradley E. Martin
UNCLASSIFIED	UNCLASSIFIED	UNCLASSIFIED	SAR	31	19b. TELEPHONE NUMBER *(Include area code)*

Moisture effects on the high strain-rate behavior of sand

Bradley E. Martin[a,*], Weinong Chen[b], Bo Song[b], Stephen A. Akers[c]

[a] *Air Force Research Laboratory, Eglin AFB, FL 32542*
[b] *Department of Aeronautics and Astronautics Engineering, Purdue University, West Lafayette, IN 47907*
[c] *U.S. Army Engineering Research and Development Center, Vicksburg, MS 39180*

Abstract

The effects of moisture content on the high strain rate mechanical properties of fine grain sand were characterized with a split-Hopkinson pressure bar. A controlled loading pulse allowed the sample to acquire stress equilibrium and a constant strain-rate of 400 s^{-1}. The sand specimen confined in a hardened steel tube, had a dry density of 1.50 g/cm^3 with moisture contents varied from 3% to 20% by weight. Experimental results indicate that partially saturated sand is more compressible than dry sand with the softest behavior observed at 7% moisture content. The softening of the partially saturated sand may occur due to the pore water acting as a lubricant between the sand particles. Similar trends were reported in the quasi-static regime for experiments conducted at comparable specimen conditions.

Keywords: Dynamic, Hopkinson bar, pulse shaping, moisture content, sand, high strain-rate

1. Introduction

Geo-materials (e.g., soils, sand, and concrete) are widely used in engineering applications ranging from military to civilian construction. For instance, in military applications soils can be used as over-burdens for protective structures. They can also affect the overpressure region associated with weapon effects (Felice et al., 1987a). Compared to metals, the mechanical properties of geo-materials tend to be less characterized and consequently less understood, in particular, when subject to high loading rates. A better understanding of the dynamic response of sand is necessary to better describe the response of soils by incorporating associated physics into constitutive models.

Predictive capabilities of current sand constitutive models are limited due to the complex nature of the material, in particular, when parameters such as loading rates, density, and moisture contents need to be considered as variables. For example, partially saturated soils under loading exhibit a multiphase behavior due to four different

* Corresponding author: Tel.: 1.850.882.6776: fax: 1.850.883.1381
E-mail address: bradley.martin@eglin.af.mil.

constituents interacting to give the overall material response (1) soil skeleton, (2) pore water, (3) grain stiffness, and (4) pore air (Hampton et al., 1966). Constitutive models will have to account for the mechanical response of these constituents and the interactions between them. Other parameters, such as stress state and grain refinement may also affect the mechanical response. A robust and accurate constitutive model will have to be multi-scale and multi-physics in nature and currently does not exist, despite the need for it in engineering applications.

High-rate applications require the sand response to be characterized at high rates. However, geo-materials are not traditionally characterized under such loading conditions. Sand, for example, has been sporadically investigated to characterize the high-rate behavior over the past three or four decades. Charlie et al. (1990) tested unsaturated 50/80 silica sand subjected to dynamic compressive loading using a conventional split-Hopkinson pressure bar (SHPB). Sand specimens were compacted and confined in a steel tube with steel wafers placed on both sides of the specimen. The primary focus was to evaluate the effects of saturation levels on the material longitudinal wave speed and transmission ratio (ratio of the transmitted stress to the incident stress). Work by Bragov et al. (1995) investigated plasticine and clay confined in a rigid steel jacket using a conventional SHPB. Composite striker bars allowed both loading and unloading of the sample to be analyzed. These experiments characterized the mechanical properties in compression at a strain-rate of 4000 s^{-1}. In earlier work Ross et al. (1986) used a conventional SHPB to evaluate a single short pressure pulse traveling through long specimens of 20/40 dry sand, 50/80 dry sand, silica flour, clay, glass beads, and steel balls. Static and dynamic compaction methods were investigated in conjunction with varying moisture contents. Pierce (1989) evaluated moisture and confining effects using a conventional SHPB for 20-30 Ottawa sand and Eglin sand. Tri-axial confining pressures were generated by applying axial pressure through the incident/transmission bars and then pressurizing water between a thin membrane and the inner wall of the confining cell for lateral confinement. The data collected included stress transmission ratios and longitudinal wave speed data for varying percent saturation levels at confining pressures of 0 kPa and 310 kPa. Felice et al. (1987a) evaluated clayey silty sand using a conventional SHPB with specimens compacted to an initial density of 1.87 g/cm^3. The clayey silty sand was evaluated at strain-rates of 500 s^{-1} to 5000 s^{-1}, achieved using different specimen dimensions and striker bar velocities. The focus was to determine if the basic assumptions used in SHPB techniques could be satisfied and if the data was repeatable. Later work by Felice et al. (1987b) conducted 26 experiments using a conventional SHPB to investigate the high strain-rate behavior of clayey sand with varying water contents, specimen dimensions, and loading stresses. Veyera (1994) studied the uniaxial stress-

strain behavior of compacted moist Eglin sand, Tyndall sand, and Ottawa 20-30 at strain rates of 1000 s^{-1} and 2000 s^{-1} using a conventional SHPB. The specimens had varying percent saturations from 0% to 100% with specimens at 20% saturation having a similar response as dry sand and percent saturations 40% and higher having a stiffer response than dry sand.

Despite these research efforts, the high-rate response of partially saturated sand is still not well understood. In some cases the results are inconclusive or even contradictory. Part of the reason is the complexity of the specimen material and the lack of standardization of the dynamic experimental methods. Due to the complex nature of the material, variations of the testing conditions inherent in the characterization methods should be kept to a minimum in order to reveal the intrinsic material response. Recent developments in SHPB techniques have significantly improved the ability to control the testing conditions the specimen experiences. For example, the conventional SHPB gives a square incident pulse with very fast initial loading rates. Fast loading rates may be acceptable when stiff materials, such as metals are investigated. However, in the case of geologic materials the longitudinal wave speeds are orders of magnitudes slower requiring a slower loading rate to allow the material to acquire stress equilibrium and constant strain-rate. In this investigation, a modified SHPB using a pulse shaping technique is used to characterize the material response of fine grain sand confined with a hardened steel tube. The testing conditions (dynamic stress equilibrium and constant strain-rate) on the specimen were controlled using shaped loading pulses. The conditions were also verified by checking the stress equilibrium and strain-rate histories for each experiment. The only parameter varied is the moisture content. Experimental results from well controlled experiments will aid in creating a quality database of dynamic properties to be used for the development of physics-based constitutive models for sand. In the following sections the experimental technique is briefly described with results presented and discussed.

2. Split-Hopkinson Pressure Bar (SPHB)

The conventional SHPB was originally developed by Kolsky (1949) and consists of three elastic rods, a striker bar, an incident bar, and transmission bar (Fig. 1). The striker bar is driven to apply an impact load on the specimen. To record the deformation and loading histories in the specimen the incident and transmission bars are introduced as sensors and load carriers. The stress waves in the elastic bars carry information characterizing the loading conditions to the bar ends (Hopkinson 1914). As instrumentation for measuring stress waves were improved and experience for conducting such instrumented experiments increasing, the basic SHPB setup has been

continuously improved over the years (Lindholm, 1963; Follansbee, 1985; Nemat-Nasser, 1991; Gray, 2000). The data reduction method using one-dimensional elastic wave theory and the assumption of stress equilibrium in the specimen has been well documented (Gray, 2000).

For ductile metallic specimens, which the SHPB was originally designed to characterize, the stress equilibrium assumption is typically satisfied. When sand is being investigated controlled experiments are necessary to ensure the specimen is deforming under valid testing conditions. This is due to sand having a very different mechanical response than metals suggesting that testing methods valid for metal characterization may not be applicable to sands. Unlike quasi-static experiments where desired testing conditions are better controlled using closed-loop control systems, control of testing conditions on specimens in SHPB experiments can be achieved mainly through controlling the impact loading pulse. The technique to generate such desired incident pulses is commonly called pulse shaping, which is described below.

Longitudinal wave speeds in soils, such as partially saturated sand, are controlled by complex interactions between sand particles, pore water, and pore air. Under dynamic compressive loading the longitudinal wave speed will vary as the compressive stress compact's the specimen material. Moisture content will also influence the longitudinal wave speed. Compared to most engineering materials, the wave speed of sand is an order of magnitude slower, as shown in Table 1. During an impact experiment for dynamic material property characterization the strain rate in the specimen has to be accelerated from zero to a desired level. The reflections of the input stress waves have varying stress levels in the specimen that provide sufficient driving force for the deformation acceleration. High wave speeds in the specimen facilitate a more evenly distributed stress field in the specimen, which is necessary for stress equilibrium. When the longitudinal wave speed is significantly low, such as that in sand, the specimen may not achieve stress equilibrium if the loading rate is high. Due to the compaction process in the specimen material, initial non-uniform deformation changes the specimen condition, thus significantly affecting the results. To facilitate a more uniform deformation from the early stages of the experiment, the initial loading rate needs to be controlled to a level that allows the stress in the specimen to be increased nearly uniformly. We used pulse shaping to serve this purpose and a dynamic stress equilibrium check to verify the effect. The loading pulses with controlled profiles also facilitate constant strain-rate deformation in the specimen after this initial acceleration.

We control the incident pulse with a pulse shaper of annealed copper with a diameter of 7.1 mm and thickness of 0.81mm. The disk is placed on the impact end of the incident bar shown in Fig. 1. The disk upon

impact with the striker bar is plastically deformed shaping the incident compressive wave. The amplitude and duration of the incident compressive wave can be controlled by a) varying the geometry of the copper disk, b) changing the striker bar velocity, and c) changing the length of the striker bar. A well shaped incident pulse produces dynamic stress equilibrium and constant strain-rate within the specimen. In a conventional SHPB experiment, e.g., on dry sand by Veyera (1994), the incident pulse is nearly trapezoidal with a loading time of approximately 25 μs, which generates a decreasing reflected pulse indicating a constantly changing strain-rate in a specimen that may have become non-uniform through the initial rapid laoding.

In this research we load the specimen with controlled pulses that allow the specimens to acquire stress equilibrium at nearly constant strain rates. Typical oscilloscope records for experiments in this research are shown in Figs. 2 & 3. Fig. 2 displays the raw data collected by the strain gages with compression being positive and tension negative. Data in Fig. 3 is obtained by truncating the incident, reflected and transmitted pulses using predetermined starting points, which will be discussed in a subsequent section. The reflected pulse is inverted with all signals plotted on the same time scale for comparison. The stress at the incident bar/specimen interface, i.e., front stress, is obtained by subtracting the reflected pulse from the incident pulse. The stress at the transmission bar/specimen interface, i.e., back stress, is determined from the transmitted pulse. The incident pulse in Fig. 3 has a loading time of approximately 125 μs with the reflected pulse showing a nearly constant strain-rate. Additionally, the stresses on the front and back ends of the specimen are similar signifying uniform deformation, as shown in Fig. 4b.

The low longitudinal wave speed in sand also limits the specimen length. A long specimen will delay stress equilibrium and cause initial non-uniform deformation. Prior to evaluating the sand a study conducted by one of the authors (Song) determined the specimen thickness required to ensure dynamic stress equilibrium within the specimen. The study investigated the same material in a dry condition using a conventional SHPB. Specimen lengths of 28.4 mm, 25.4 mm, 15.2 mm, and 13.1 mm confined in polycarbonate tubes were investigated. The experiments showed that stress equilibrium is achieved earlier with a thinner specimen. High speed digital images obtained using a Cordin camera for specimen thicknesses of 28.4 mm and 13.1 mm and are shown in Fig. 4. These images were taken at the mid-point of the stress-strain curve. The 28.4 mm long specimen shows a compaction wave propagating in the specimen indicating non-uniform deformation. However, the 13.1 mm specimen is deformed uniformly along the entire length of the specimen. These images also show that uniform deformation is

more obtainable as the specimen thickness decreases. From analysis of these images, Song suggested a specimen thickness of 9.3 mm be used when a conventional SHPB is used for sand evaluation. Beside the rapid initial loading rates, incident pulses in a conventional SHPB have Pochammer-Chree high frequency oscillations (Felice et al., 1987a). These high frequency oscillations cause variations in strain-rate and non-uniform deformation, thus creating uncertainties within the stress-strain response. These undesired high-frequency oscillations can be eliminated and a constant strain-rate within the specimen obtained through pulse shaping.

3. SHPB Experiments

3.1. Modified SHPB

Shown in Fig. 1, the SHPB used in this investigation consists of a striker bar, an incident bar, a transmission bar, a copper pulse shaper and a sample sandwiched between the incident and transmission bars. Compressed air released using a fast acting valve launches the striker bar into the incident bar creating an compressive wave that travels down the incident bar towards the sample. Since the impedance of the sand specimen is less than that of the bars, part of the compressive wave propagates through the specimen to the transmission bar and part is reflected back into the incident bar as a tensile wave. The incident stress wave contains no high-frequency components, enabling it to propagate along the bar without dispersion and then deforming the specimen uniformly. The nearly non-dispersive waves measured at strain gage locations on the bar surfaces away from the specimen can be used to determine the specimen response. Strain gages mounted on the incident bar measure the incident, ε_i, and reflected, ε_r, strains and gages mounted on the transmission bar measure the transmitted strain, ε_t. The data reduction method is based on the one-dimensional wave theory and is well documented by Gray (2000).

Shown in Fig. 1 the incident and transmission bars have density ρ, area A, Young's modulus E, and wave speed c_0. The subscripts *i, r, t* designate the incident, reflected and transmitted waves, respectively. Due to the nature of the compression tests, the stress is taken positive in compression, strain positive in contraction, and velocity positive in the right direction. Quantities associated with the specimen are identified by a subscript "s", with 1 and 2 indicating the front and back of the specimen respectively. The front and back stress of the specimen is given by the following equations (Gray, 2000).

$$\sigma_1 = \frac{A}{A_s} E(\varepsilon_i + \varepsilon_r) \tag{3a}$$

$$\sigma_2 = \frac{A}{A_s} E(\varepsilon_t) \tag{3b}$$

These relations allow direct verification of stress equilibrium by comparing σ_1 and σ_2 obtained from experiments. If a state of dynamic stress equilibrium exists, where the stresses on both sides of the specimens are equal $\sigma_1=\sigma_2$, then specimen stress, strain-rate, and strain can then be derived using the strain signals measured from the bar surface.

$$\sigma_s = \frac{A}{A_s} E\varepsilon_t \tag{4}$$

$$\dot{\varepsilon}_S = \frac{2c_o}{l_s} \varepsilon_r \tag{5}$$

$$\varepsilon_S = \frac{2c_o}{l_s} \int_o^t \varepsilon_r dt \tag{6}$$

The striker, incident and transmission bars in Fig. 1 were fabricated of VM C350 maraging steel (HRC = 53) with a yield strength, Young's Modulus and density of 2.5 GPa, 200 GPa, and 8100 kg/m^3, respectively. The bars have a common diameter of 19.1 mm with the ends of the bars faced to length and polished. The lengths of the striker bar, incident bar and transmission bar for these experiments were 685 mm, 4150 mm, and 2440 mm, respectively. Diametrically opposed strain gages were located on the incident bar and transmission bar to nullify bending strains in the bar. The strain gages were located approximately 1300 mm from the specimen on the incident bar and approximately 200 mm from the specimen on the transmission bar. Each set of strain gages are connected to form a Wheatstone bridge excited by a 24 V power supply. Finally, the signal is conditioned by a pre-amplifier and recorded with a high speed digital oscilloscope.

3.2. Specimen Preparation

The material investigated in this study is silica based fine grain sand, kiln dried, and poorly graded (ASTM, 2001). The geometric sand properties are documented in Table 2 with the gradation shown in Fig. 5. The dynamic compressive response of the sand was investigated in this study at various moisture contents ranging from 3% to 20% by weight with all specimens having a dry density of 1.50 g/cm^3. All specimens were in an undrained condition, where water or air is not allowed to escape. The specimens were confined using a hardened 4340 steel

tube with an outer diameter of 25.4 mm, inner diameter of 19.1 mm and length of 50.8 mm. The steel tube is used to achieve high confinement levels and to replicate a uniaxial strain condition.

A pair of holes are drilled in the steel tube 14.8 mm from the end, 180 degrees apart. Two 6.35 mm thick steel platen are placed in the steel tube and between the incident and transmission bars. Knowing the thickness of the specimen, striations are marked on the incident and transmission bars at 14.0 mm and 14.8 mm, respectively, from the end of each bar. One steel platen is then held in place in the steel tube with the incident and transmission bars. The steel tube is then slid back and forth to ensure movement of the platen is not hindered. The steel tube is then aligned with the striation on the transmission bar and the steel platen held in place by a set screw. The steel tube is removed from the SHPB and placed vertically on top of a 19.1 mm diameter rod fixture. A piece of paper is placed on top of the scale, tared and 4.0 g of sand weighed. The sand is poured into the steel tube and tapped lightly to even the top surface. Using a 1ml syringe, the appropriate weight percent (e.g., 0.28 ml for 7% moisture) of water is obtained and all air voids removed from the syringe. The water is slowly released from the syringe into the dry sand and evenly distributed over the top of the sand. The sand and water are mixed to acquire a uniform distribution of water. The second steel platen is then placed on top of the partially saturated sand and slightly pressed to ensure the interface between the platen and partially saturated sand is flat. The assembled specimen is shown in Fig. 6. The steel tube is removed from the rod fixture and carried vertically to the SHPB. One drop of cyanoacrylate is placed on the incident bar and spread over approximately 70% of the bar diameter. This ensures the steel platen is held in place when the reflected tensile wave arrives at the incident bar/steel platen interface. Holding the top steel platen with fingers the specimen is turned horizontally and placed between the incident and transmission bars with the cyanoacrylate allowed to dry. Light pressure is applied to the incident and transmission bars until the end of the steel tube is aligned with the incident bar striation. The initial specimen length is then computed as 50.8 – 14.0 – 14.8 – (6.35 x 2) = 9.3 mm. The set screws are removed prior to stress wave loading of the specimen. Following each experiment the steel confinement tube and steel platens are cleaned to remove excess sand and cyanoacrylate. The steel confinement and steel platens were reused for subsequent experiments

4. Experimental Results

High strain rate experiments were conducted on fine grain sand specimens with a nominal diameter of 19.1mm and nominal length of 9.3 mm, corresponding to an aspect ratio (L/D) of 0.49. A total of 43 experiments were conducted with a strain-rate of approximately 400 s^{-1}. All specimens were confined by a steel tube with

moisture contents varying from 3% to 20% by weight. A minimum of five experiments were conducted at each moisture content, except at 5% moisture content where four experiments were conducted, to investigate the repeatability of the data.

One-dimensional wave theory is used to reduce all data collected from the modified SHPB experiments. The starting point of the reflected pulse, following the incident pulse, was obtained by using the longitudinal wave speed of the incident bar material (~5,080 m/s) to calculate the time required for the incident pulse to travel from the strain gage to the specimen, be reflected at the bar/specimen interface, and travel back to the strain gage. This time is $T = 2L/C_o$, where L is the distance from the strain gage center to the bar/specimen interface and C_0 is the wave speed of the incident bar material. The starting point for the transmitted signal was computed in a similar fashion. The starting point of the transmitted pulse is calculated using: $T = T_s + T_t + 1/2\,T_r$ where T_s is the transit time through the specimen, T_t is the time to travel from the specimen to the transmission bar strain gage and T_r the transit time for the reflected pulse. The transit time for the stress wave to propagate through the specimen is calculated using the strain gage records and the difference between the starting times for the reflected and transmitted pulses and subtracting out the time for the stress wave to travel to its appropriate strain gage on the incident and transmission bars. Using this method the calculated longitudinal wave speed for the specimen is approximately 300 m/s, which is within the range reported by Charlie et al. (1990) in Table 1. The calculated starting times for the reflected and transmitted pulses are 1060 μs and 640 μs, respectively. These times were used in reducing data for all experiments in this investigation.

To illustrate the repeatability of the experiments, all five stress-strain curves for 7% moisture content are shown in Fig. 7. A two sigma standard deviation was calculated using the five stress-strain curves in Fig. 7 for percent strains of 1, 3, 5, 7, & 8. The mean stress-strain curve with standard deviation for 7% moisture content is shown in Fig. 8. The mean dry sand stress-strain response in Fig. 9 was determined in the same fashion, but the bars only represent the maximum and minimum stresses obtained at the corresponding percent strain not a standard deviation. To examine the repeatability with a larger sample size, one of the authors (Song) conducted 30 experiments with an approximate strain-rate of 470 s^{-1}, used the same sand material at dry conditions, modified SHPB, and specimen preparation method. They found the error range to be very similar to that shown in Fig. 9. The mean stress-strain curves for each moisture content show significant oscillations in stress between 2% to 4%

strain. Oscillations are not evident for the dry sand mean stress-strain curve, but some of the 30 experiments conducted by Song show similar oscillations. The mean stress-strain relationships under steel confinement for this investigation are shown in Fig. 9. For all experiments, the stress-strain curves are truncated at the maximum percent strain where both stress-equilibrium and constant strain-rate conditions are satisfied. The mean curves in Fig. 9 represent the family of stress-strain curves at each moisture content.

The results in Fig. 9 show that after the sand specimens are initially compacted, the oscillations in the stress-strain curves diminishes after a strain of 4%. The stress-strain behavior of the sand at all moisture contents is remarkably linear up to the strain of 8% to 9% when unloading initiates in the experiments with partially saturated sand. The dry sand results show the highest slope, corresponding to the stiffest behavior. As water is added progressively from 3% to 5% to 7% the stiffness decreases with increasing water content. As the water content is further increased, the sand specimen behavior stiffens. However, all the partially saturated sand is less stiff compared to dry sand with specimens at 7% moisture content having half the stiffness of dry sand.

5. Discussion

5.1. Moisture Effects

The porosity of a given particulate material is dependent on the shape of the particles and the particles size distribution. Dry sand can be considered as two-phase material: a solid corresponding to the sand skeleton and a gas associated with the pore air. If water or any other liquid is added then it is a three phase material unless it is fully saturated.

In our investigation, the specimen consists of a sand skeleton and pores filled with air and water in an undrained state. If the specimen is strained sufficiently, all pore air or pore water will be removed form the volume if drained conditions prevail, but in undrained conditions pore air and pore water are displaced without leaving the volume. When all pore air is replaced by pore water the specimen is fully saturated and water is loaded causing the specimen to stiffen with little additional compression of the specimen. The experiments conducted in this investigation use steel confinement to contain the specimen. This condition preferentially allows axial strain to occur, since radial stress generated by the steel confinement will constrict lateral expansion. For uniaxial strain conditions the volume fraction of air voids in the specimen is directly related to the percent strain required to remove the air voids. When the percent strain is equal to the maximum percent volume of air, it can be assumed that the specimen is fully saturated. The corresponding percent volume of air associated with each of the investigated

moisture contents is tabulated in Table 3. In the series of experiments reported in this paper, the specimens were loaded to approximately 9% strain. With the maximum percent strains below the maximum percent volume of air voids the effects of water are not dominant. The mean stress-strain curves in Fig. 9 show no evidence of the material "locking up" where the specimen becomes completely saturated and water is loaded.

For the low strains in Fig. 9 one might expect the material response of the dry and partially saturated sand to be similar since pore air is still within the specimen. The data suggest that when compressing partially saturated sand at high strain-rates the interaction between the sand particles, pore air and pore water respond differently than under dry conditions. One interpretation of these results is that higher levels of friction exist at the sand particle interface in dry sand. The presence of water provides a degree of hydrostaticity and has the net effect of reducing friction in partially saturated sand. The presence of hydrostaticity will lower the shear stress between the particles and in the system. As the specimen is compressed pore air is displaced enabling sand particles to rearrange themselves in the presence of water. This phenomenon may be better explained by concentrating on the partially saturated sand responses. As indicated in Fig. 9 the stiffness of the stress-strain response decreases as the moisture content changes from dry sand to 3% thru 7% partially saturated sand. At approximately 9% the stiffness increases gradually up to 20% moisture content. For low moisture contents water concentrates in the inter-particle contact areas occupying less pores, enabling the displacement of pore air and allowing sand particles to move freely making the specimen more compliant. It is possible that there is pore connectivity. However, at higher moisture contents more water occupies the pores within the specimen prohibiting large displacements of air. This keeps sand particles from moving and stiffens the specimen back up. Although a small trend in changes in stiffness is evident the differences are indistinguishable from one another (with the large uncertainty in reproducibility) indicating that small changes in moisture content did not significantly affect the stiffness of partially saturated sand. Also as indicated in Table 3 at higher concentrations of moisture content, it is still a three phase system.

Another explanation of the moisture effects on the dynamic behavior is related to the boundary conditions between the steel platen and specimen. The water could be acting as a lubricant between the specimen and steel platens. This lubrication effect is not present in the dry sand experiments. Assessing the contribution of the boundary conditions on the material response would require development of new techniques with sufficient resolution that allows insitu measurements of particle motion at the boundary. Such techniques and data are currently not available.

5.2. Comparison of experiments

Quasi-static uniaxial strain tests have been accepted as well controlled experiments with well defined boundary conditions. In this section, results of quasi-static uniaxial strain experiments for dry and partially saturated sand conducted with the same boundary conditions and material are qualitatively compared to the results in this investigation.

A uniaxial strain test loads the specimen in the axial direction and constrains the specimen in the lateral direction with the radial loading and displacement recorded. The assembled specimen is shown in Figs. 10 & 11. The specimen has three membranes placed around the specimen with the outer membrane coated with liquid synthetic rubber to prohibit deterioration from the confining fluid (Williams et al., 2006). The specimen is mounted with a Linear Variable Differential Transformer (LVDT) (Fig. 11) to measure the axial strain. A lateral deformeter is mounted at the specimen mid height to measure radial displacement. The lateral deformator has a LVDT mounted to a hinged ring so as the specimen is displaced radially the ring opens measuring the displacement. The specimen is placed in a pressure vessel where a confining fluid is used to provide lateral confinement while axial loading is provided by a servo controlled piston. Additional information on the execution and instrumentation used for the uniaxial strain experiments is reported by Williams et al., 2006.

All quasi-static uniaxial strain experiments for both dry and partially saturated sand were studied under comparable specimen conditions, using the experimental technique reported by Williams et al., 2006. The specimens were 50 mm in diameter and 110 mm in length having an aspect ratio of 2 compared to an aspect ratio of 0.49 for the specimens in this investigation. The specimens had an average dry density of 1.651 g/cm^3 for both the dry and partially saturated experiments. The dry sand had a post-test moisture content of 0.5% with the partially saturated sand having a post-test moisture content of approximately 7.0%. All experiments were conducted at strain-rates of approximately 10^{-4} s^{-1} to 10^{-5} s^{-1}. The dry density is higher than the dry density in our studies, so only a qualitative verification of trends is appropriate. The uniaxial stress-strain response data for dry and partially saturated sand are shown in Fig. 12. These data indicate that partially saturated sand is more compliant than dry sand which is consistent with the results obtained in this study.

6. Conclusions

The research documented in this report gives a comprehensive study of the material response of dry and partially saturated sand dynamically loaded at a strain rate of 400 s^{-1}. The data in Fig. 9 shows that partially

saturated sand is more compliant than dry sand. Quasi-static uniaxial strain experiments with comparable specimen conditions are in qualitative agreement. The softening of partially saturated sand is attributed to the heterogeneity of the material through complex interactions between the sand particles, pore air, and pore water. To truly understand these interactions and its effects on the physical behavior of the material quantitative insitu measurements are necessary. With current limitations in experimental techniques only qualitative conclusions concerning the material response are given below.

1. The results show that partially saturated sand is more compliant than dry sand. It is presumed that pore water acts as a lubricant at the inter-particle contact areas, decreasing the friction between the particles resulting in lower localized shear stresses.

2. The trend present in the partially saturated sand is caused by interactions between the pore air and pore water. At the lower moisture contents less water is added leaving more pore air in the specimen allowing the sand particles to move during compression. The displacing of the pore air between the particles enables the specimen to become more compliant. Subsequently, when the moisture content increases less pore air is available for displacement during compression acting to stiffen the specimen. The movement of sand particles, the lubrication of water, and increased hydrostaticity are all integrated phenomena that work together to influence the behavior of partially saturated sand.

3. An experimental uncertainty is the effect of friction between sand particles and both the steel confinement and steel platens. Frictional effects would increase the magnitude of the stress, yet this quantity is difficult to determine.

4. Significant high frequency oscillations were observed in the partially saturated sand response. These oscillations though unexplainable are repeatable and need to be further investigated by experimentally assessing the boundary effects and loading between individual particles. It is quite evident that these result from heterogeneity that is present for this class of materials.

The results are encouraging and promising in obtaining measurements for the dynamic mechanical properties of partially saturated sand for future constitutive laws. We have attempted to explain the inter-particle behavior as described above. However, to quantify the above assumptions, it will be necessary to conduct mesoscale simulations treating dry sand as a two phase material and partially saturated sand as a three phase material. This we believe very strongly is a critical link in the investigation because it has the potential to “identify” physical mechanisms that may be relevant in this discussion. This will be the subject of future research.

Furthermore, the repeatability of the data must be improved by implementing quantifiable specimen preparation and evaluation methods. A comprehensive constitutive law for sand requires controlled dynamic experiments under triaxial confinement conditions to be conducted, to enable dynamic shear properties of the material to be determined at varying stress states. This will also be the subject of future research.

Acknowledgements

This work was supported by the DoE/DoD TCG-XI through a Memorandum of Understanding with Sandia National Laboratories. Sandia supported this work through a grant with Purdue University. Sandia is a multiprogram laboratory operated by Sandia Corporation, a Lockheed Martin Company, for the United States Department of Energy under Contract DE-ACO4-94AL8500. This author appreciates the insightful conversations with Mr. Mark L. Green of the Air Force Research Laboratory.

References

ASTM, 2001. Annual Book of ASTM Standards – Soil and Rock, Section 4, Volume 04.08, Standard D2487, Conshohocken, PA.

Bragov, A.M., Grushevsky, G.M., Lomunov, A.K., 1996. Use of the Kolsky Method for Confined Tests of Soft Soils. Exp. Mech. 36(3), 237-242.

Brown, J.L., Vogler, T.J., Chhabildas, L.C., Reinhart, W.D., Thornhill, T.F., 2007. Shock Responses of Dry Sand. SAND2007-3524, Sandia National Laboratories, Albuquerque, NM.

Charlie, W. A., Ross, C.A., Pierce, S.J., 1990. Split-Hopkinson Pressure Bar Testing of Unsaturated Sand. Geotechnical Testing Journal GTJODJ 13(4), 291-300.

Craig, R.F., 1987. Soil Mechanics. 4th Edition, Chapman & Hall, 2-6 Boundary Row, London SE1 8HN, UK.

Davies, R. M., 1948. A Critical Study of the Hopkinson Pressure Bar. Philos. Trans. R. Soc. London, Ser. A 240, 375-457.

Felice, C. W., Gaffney, E.S., Brown, J.A., Olsen, J.M., 1987a. Dynamic High Stress Experiments on Soil. Geotechnical Testing Journal GTJODJ 10(4), 192-202.

Felice, C. W., Brown, J.A., Gaffney, E.S., Olsen, J.M., 1987b. An Investigation into the High Strain-Rate Behavior of Compacted Sand Using the Split-Hopkinson Pressure Bar Technique. Proceedings of the 2nd Symposium on the Interaction of Non-Nuclear Munitions with Structures, Panama City Beach, FL**,** 391-396.

Follansbee, P. S., 1985. The Hopkinson Bar. ASM Handbook, Materials Park, OH. 8, 198-207.

Frew, D. J., Forrestal, M.J., Chen, W., 2002. Pulse Shaping Techniques for Testing Brittle Materials with a Split Hopkinson Pressure Bar. Exp. Mech. 42(1), 93-106.

Frew, D. J., Forrestal, M.J., Chen, W., 2005. Pulse Shaping Techniques for Testing Elastic-plastic Materials with a Split Hopkinson Pressure Bar. Exp. Mech. 45(2), 186-195.

Gray III, G. T., 1997. High-Strain-Rate Testing of Materials: The Split-Hopkinson Pressure Bar. LA-UR-97-4419, Los Alamos National Laboratory**,**. Santa Fe, NM.

Gray III, G. T., 2000. Classic Split-Hopkinson Pressure Bar Testing. Mechanical Testing and Evaluation, Metals Handbook, American Society for Metals, Materials Park, OH. 8, 462-476.

Gray III, G. T., Blumenthal, W.R., 2000. Split-Hopkinson Pressure Bar Testing of Soft Materials. Mechanical Testing and Evaluation, Metals Handbook, American Society for Metals, Materials Park, OH. 8, 488-496.

Hampton, D., Wetzel, R.A., 1966. Stress Wave Propagation in Confined Soils. AFWL-TR-66-56, Air Force Weapons Laboratory, Kirkland AFB, NM.

Hopkinson, B., 1914. A Method of Measuring the Pressure Produced in the Detonation of High Explosives or by the Impact of Bullets. Philos. Trans. R. Soc. London, Ser. *A*, 213, pp. 437-456.

Kolsky, H., 1949. An Investigation of the Mechanical Properties of Materials at very High Rates of Loading. Proc.R. Soc. London, Ser. B 62, 676-700.

Lindholm, U. S., 1964. Some Experiments with the Split Hopkinson Pressure Bar. J. Mech. Phys. Solids, 12, 317-335.
Nemat-Nasser, S., Isaacs, Jon B., Starrett, John E., 1991. Hopkinson Techniques for Dynamic Recovery Experiments. Proc. R. Soc. London, Ser. A, A435, 371-391.
Pierce, S. J., 1989. High Intensity Compressive Stress Wave Propagation through Unsaturated Sands. Master Thesis, Colorado State University, Fort Collins, Co.
Ross, C. A., Nash, P. T., Friesenhahn, G.J., 1986. Pressure Waves in Soils Using a Split-Hopkinson Pressure Bar. ESL-TR-86-29, Air Force Engineering and Services Center, Engineering and Services Laboratory,Tyndall AFB, FL.
Veyera, G. E., 1994. Uniaxial Stress-Strain Behavior of Unsaturated Soils at High Strain Rates. WL-TR-93-3523, Wright Laboratory, Flight Dynamics Directorate, Tyndall AFB, FL.
Williams, E.M., Akers, S.A., Reed, P.A., 2006. Laboratory Characterization of SAM-35 Concrete. ERDC/GSL TR-06-15, U.S. Army Engineering Research and Development Center, Geotechnical and Structures Laboratory, Vicksburg, MS.

Figure Captions

Figure 1: Arrangement of the modified split Hopkinson Pressure Bar implementing pulse shaping

Figure 2: Voltage versus time plots using the modified split Hopkinson Pressure Bar.

Figure 3: Voltage versus time history for the experiments herein using the modified split Hopkinson Pressure Bar.

Figure 4: Sand specimen dynamic deformation: a) 28.4 mm thick specimen b) 13.1 mm thick specimen

Figure 5: Gradation curve for Quikrete #1961 fine grain sand.

Figure 6: Detailed schematic of Sand specimen confined in a 4340 steel tube.

Figure 7: Stress-strain curves for 7% moisture content.

Figure 8: Mean stress-strain curve for 7% moisture content with standard deviation.

Figure 9: Mean stress-strain curves for Quikrete #1961 sand with steel confinement. Dry sand data reported by Bo Song.

Figure 10: Schematic of uniaxial strain specimen assembly (Williams et al., 2006).

Figure 11: Photograph of the uniaxial strain specimen assembly with instrumentation (Williams et al., 2006).

Figure 12: Quasi-static uniaxial strain stress-strain data.

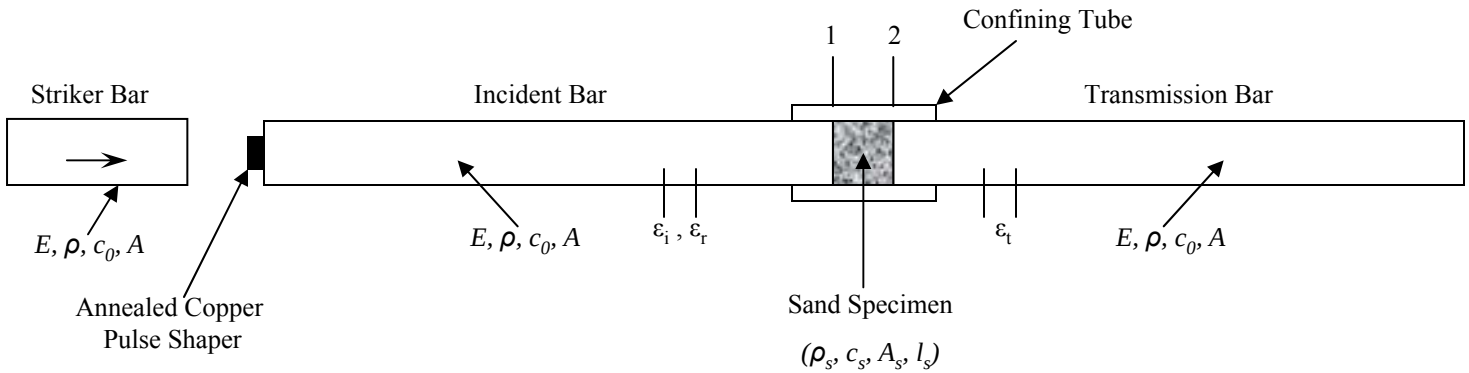

Figure 1. Arrangement of the modified split Hopkinson Pressure Bar implementing pulse shaping

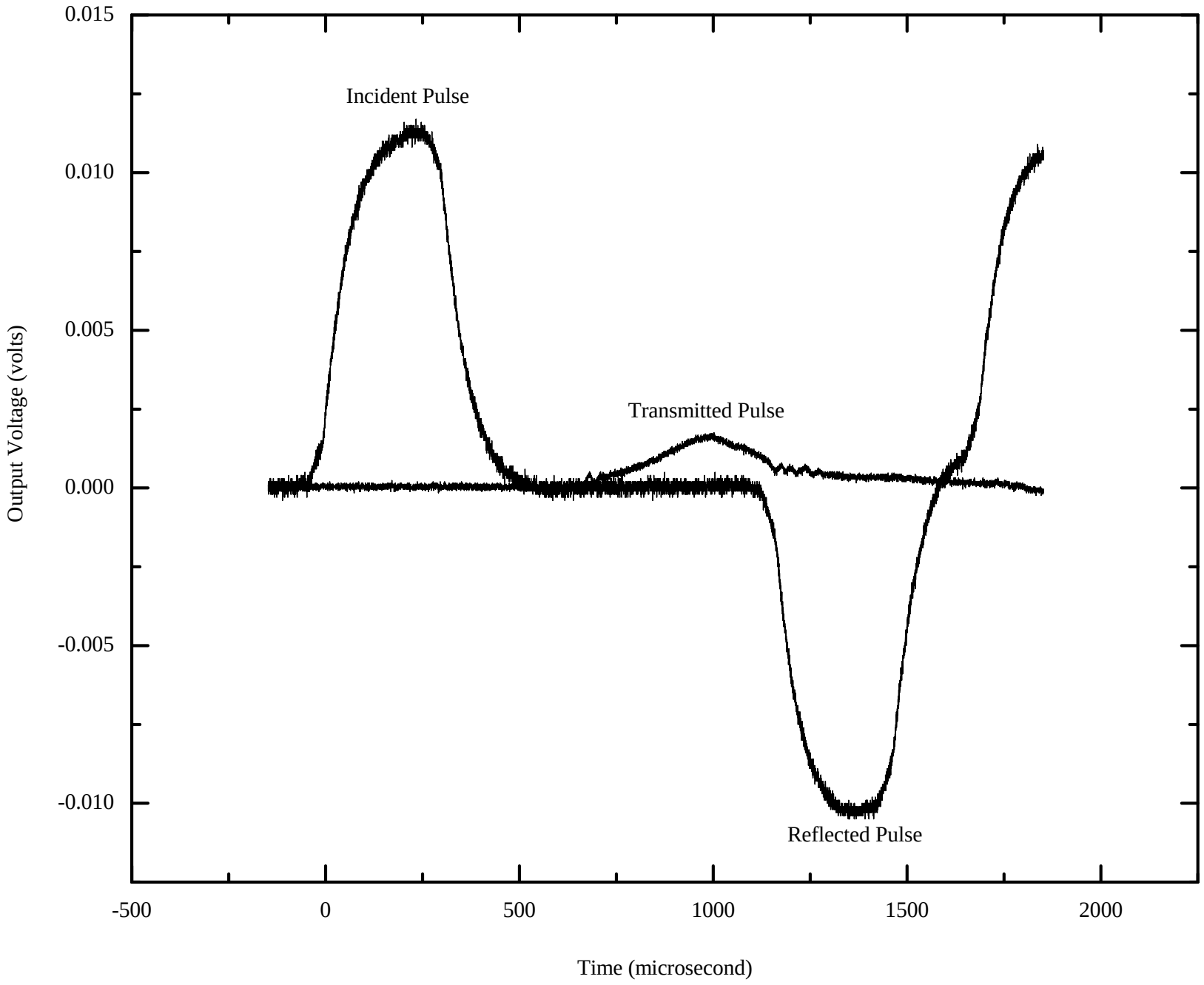

Figure 2. Voltage versus time plots using the modified split Hopkinson Pressure Bar.

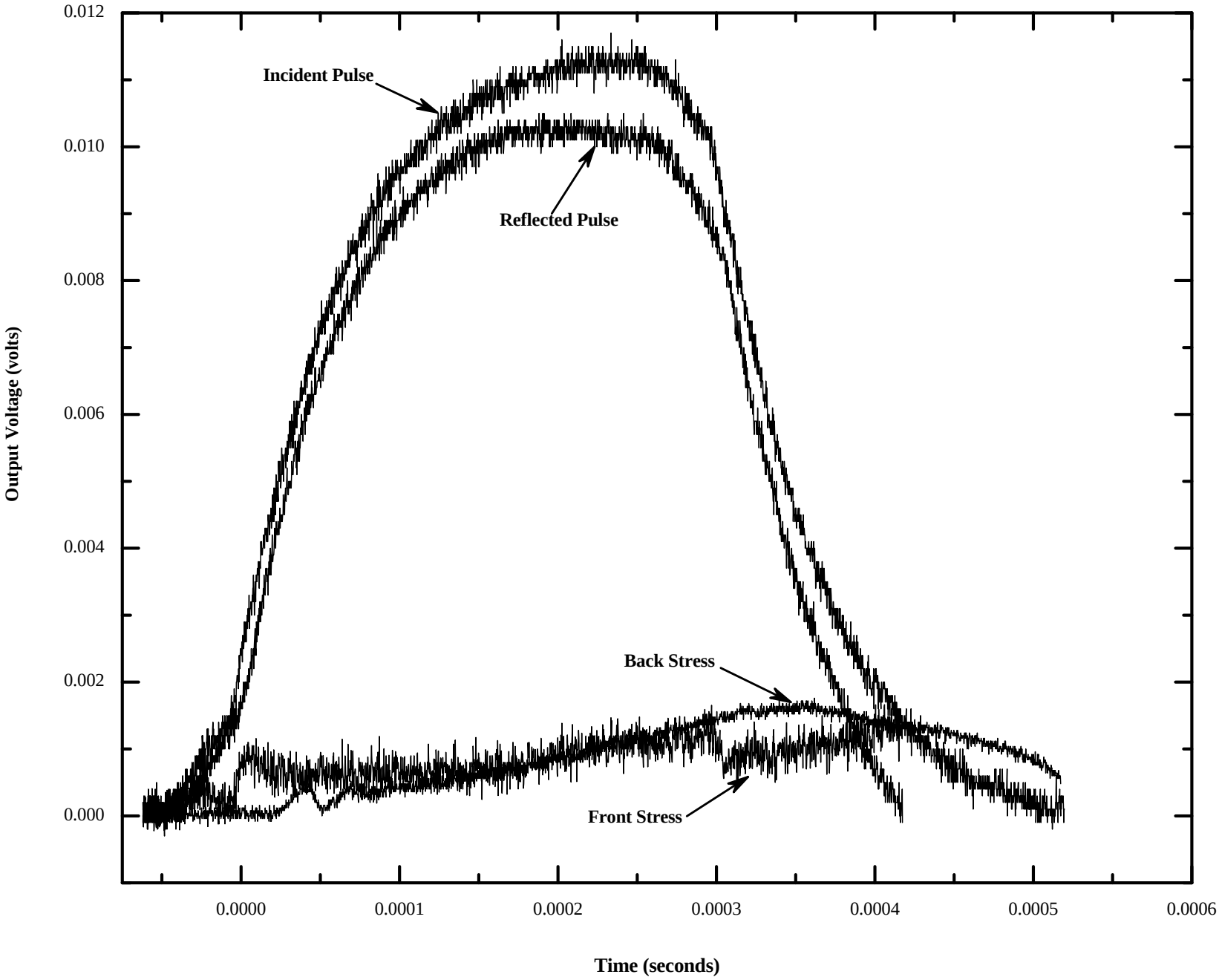

Figure 3. Voltage versus time history for the experiments using the modified split Hopkinson Pressure Bar.

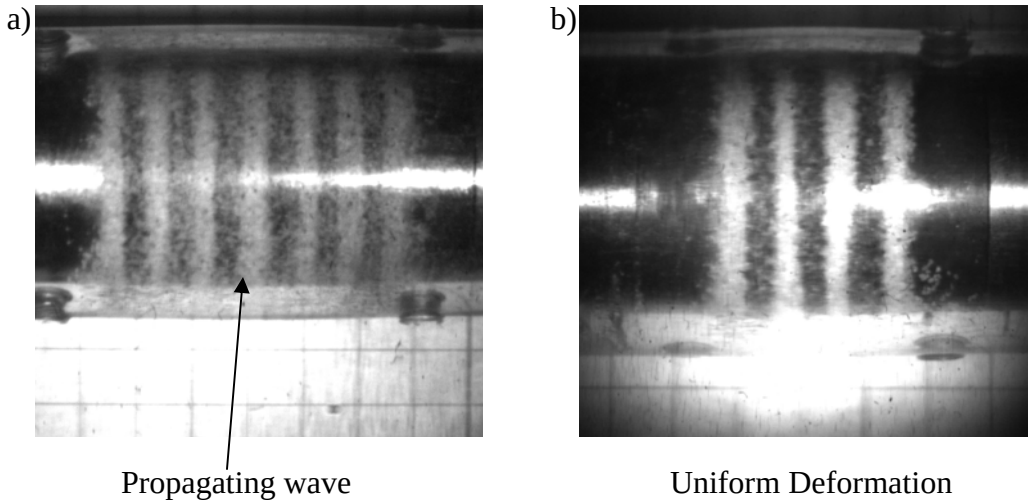

Figure 4: Sand specimen dynamic deformation: a) 28.4 mm thick specimen b) 13.1 mm thick specimen

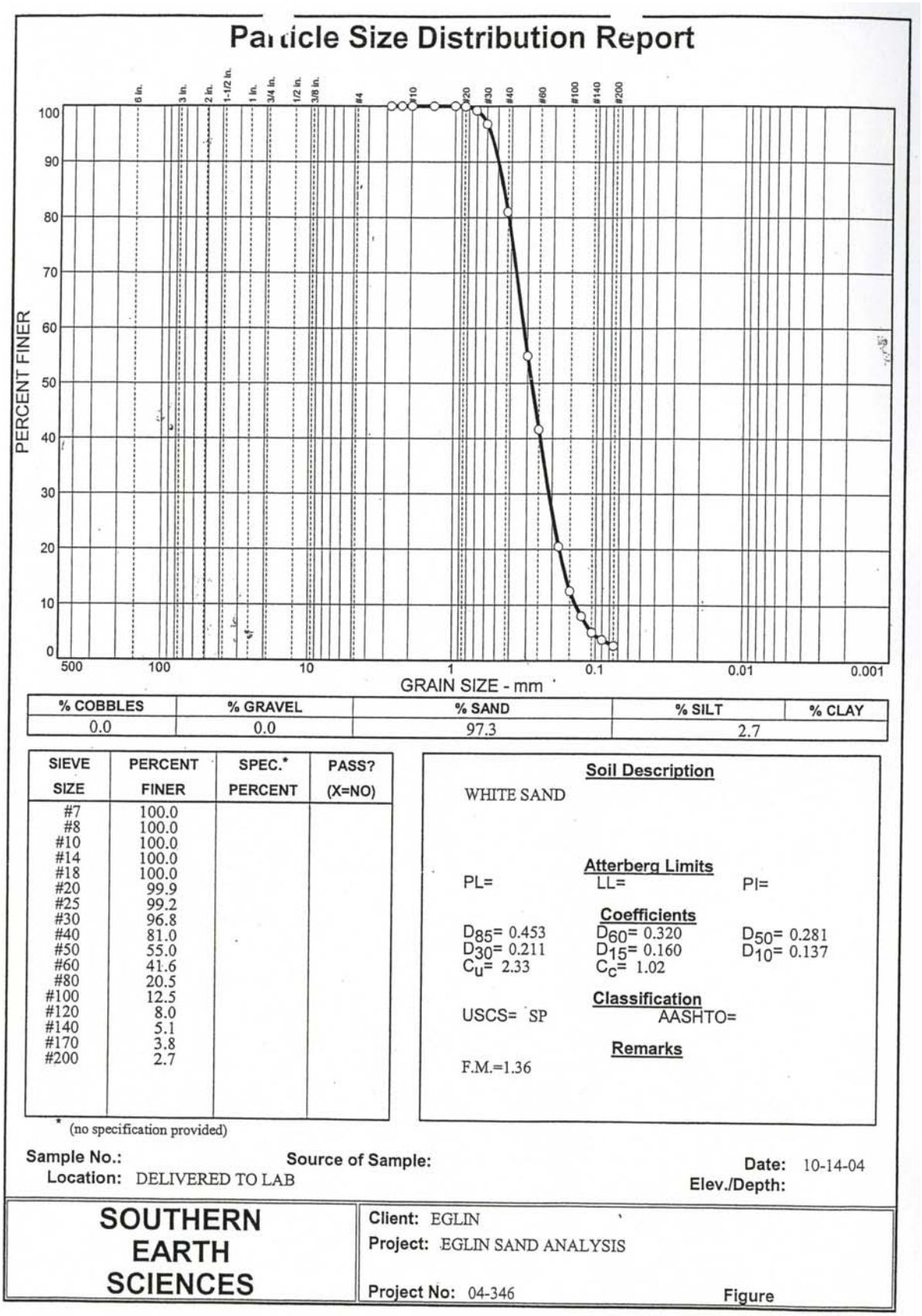

Figure 5. Gradation curve for Quikrete #1961 fine grain sand.

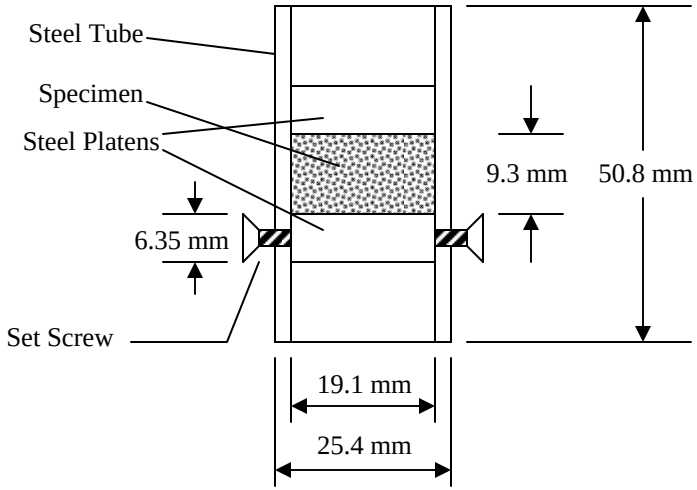

Figure 6. Detailed schematic of sand specimen confined in a 4340 steel tube.

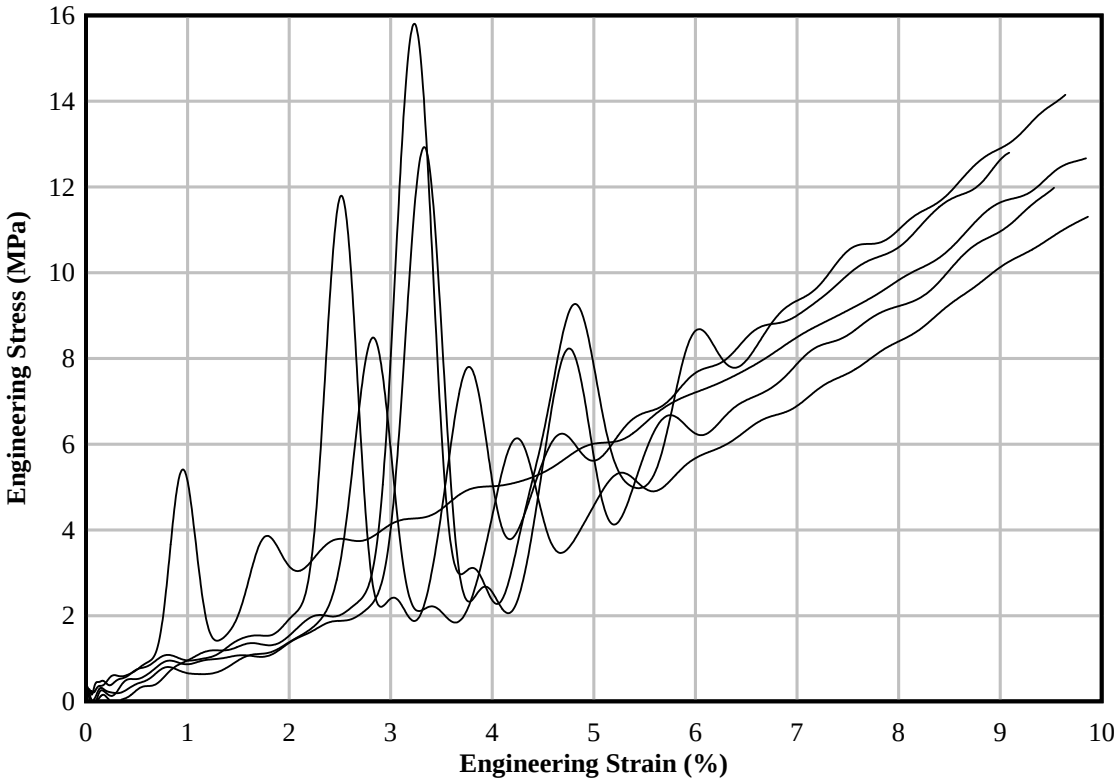

Figure 7: Stress-strain curves for 7% moisture content.

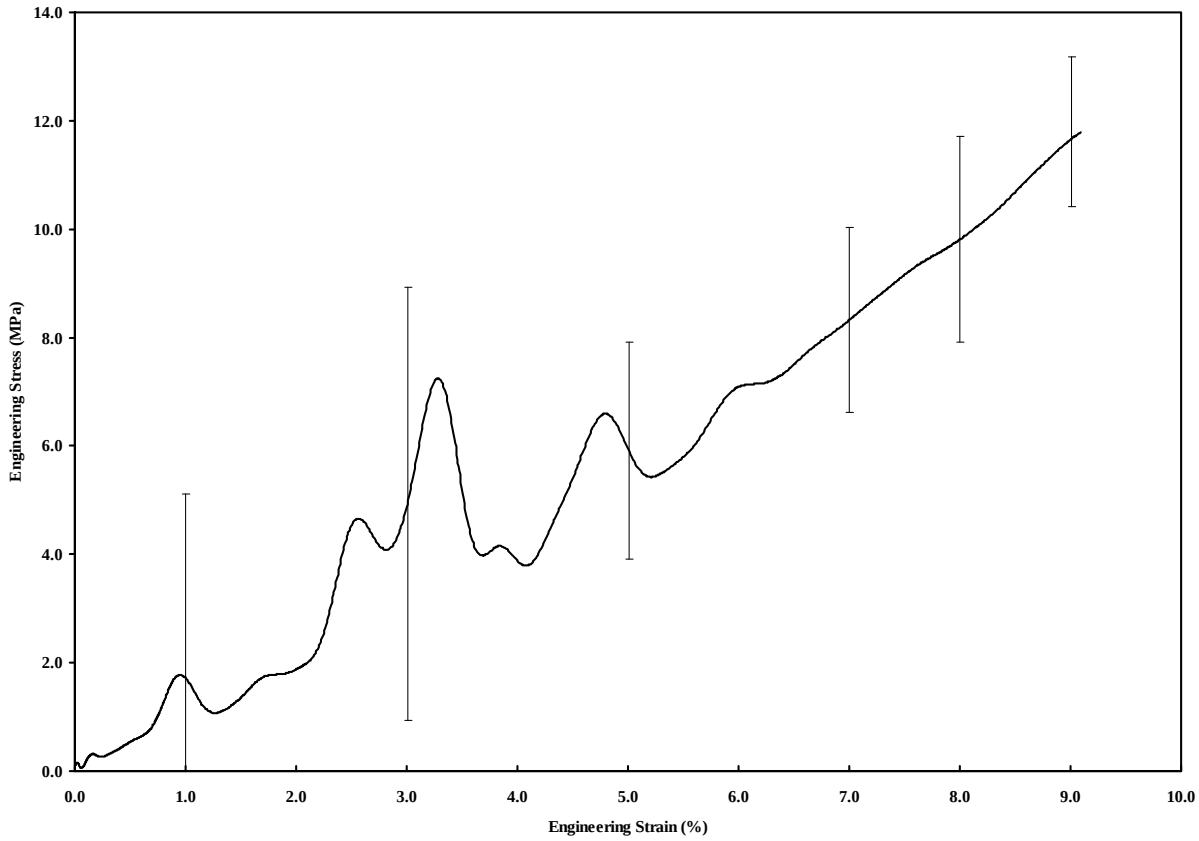

Figure 8: Mean stress-strain curve for 7% moisture content with standard deviation

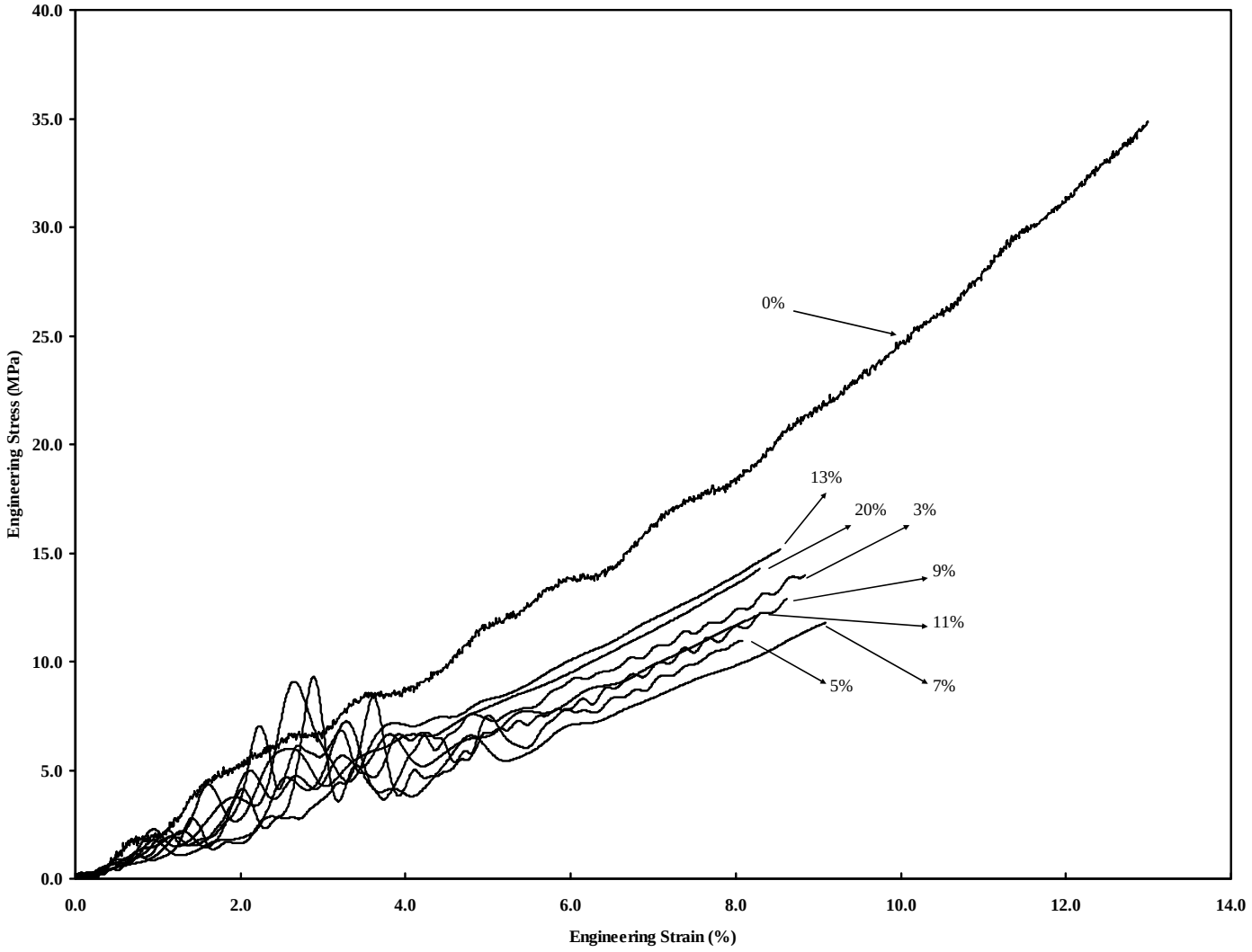

Figure 9. Mean stress-strain curves for Quikrete #1961 sand with steel confinement. Dry sand data supplied by Bo Song.

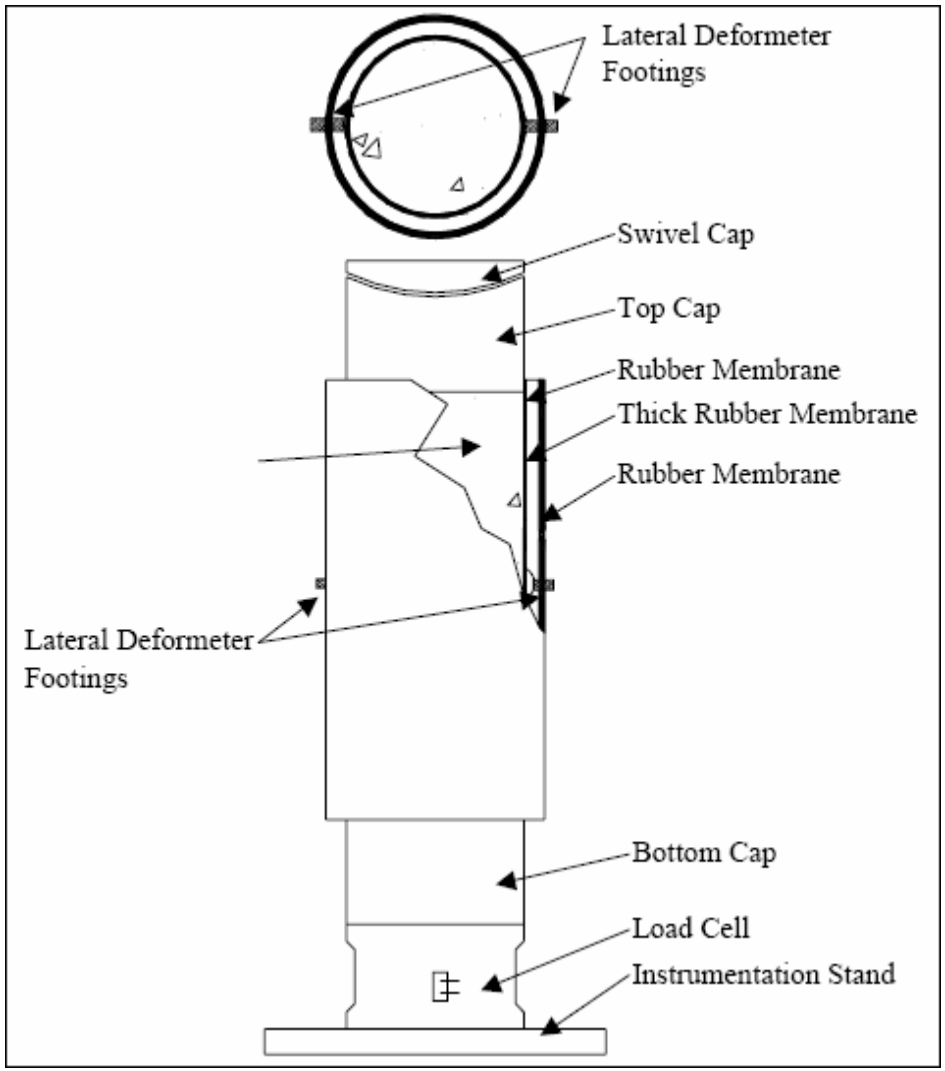

Figure 10. Schematic of uniaxial strain specimen assembly (Williams et al., 2006).

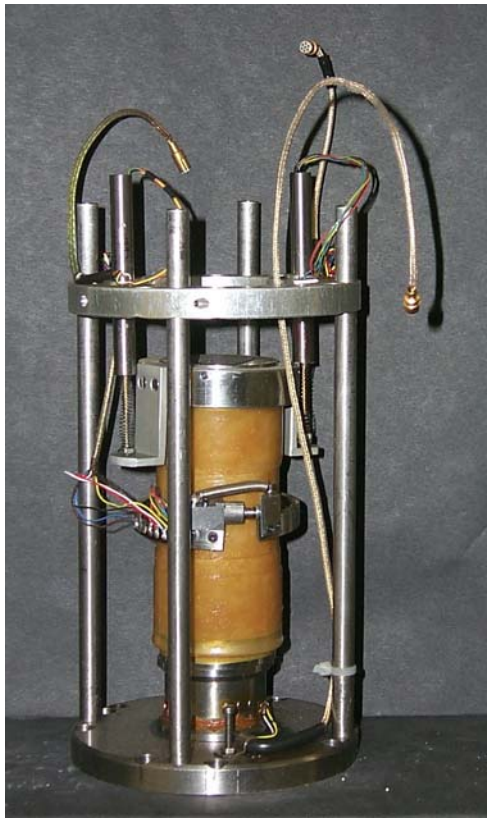

Figure 11. Photograph of the uniaxial strain specimen assembly with instrumentation (Williams et al., 2006).

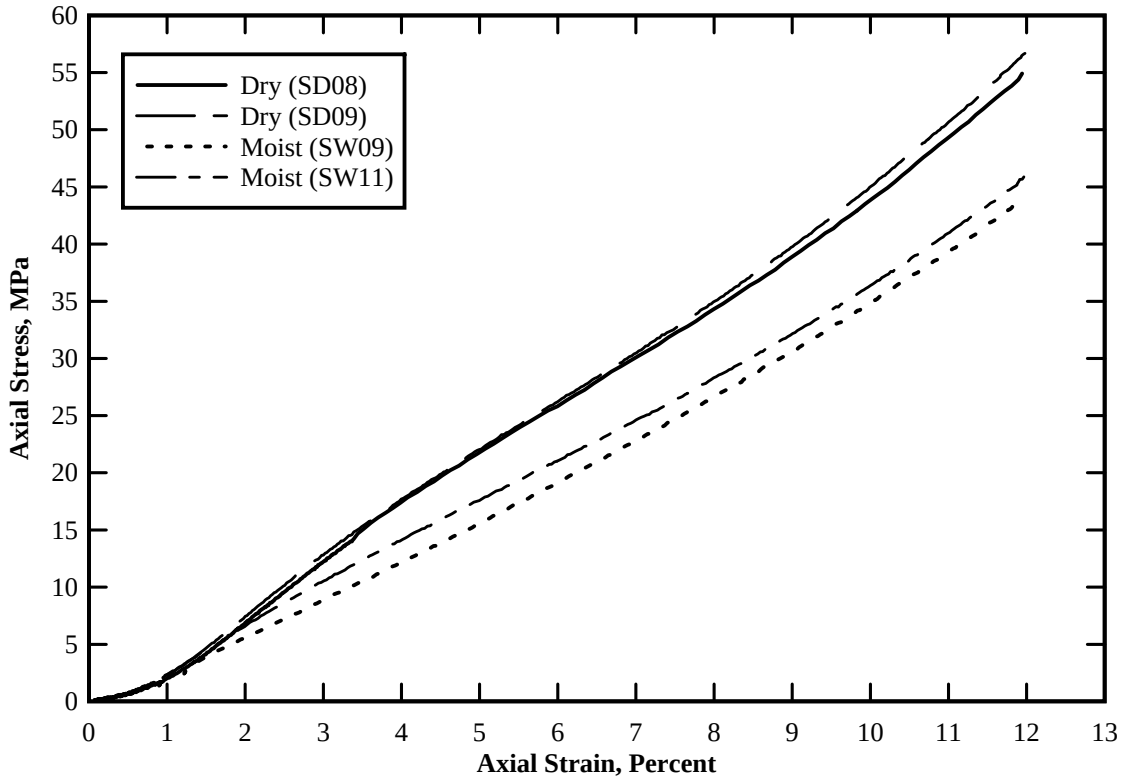

Figure 12: Quasi-static uniaxial strain stress-strain data.

Table 1
Material longitudinal wave speeds

Material	Wave Speed (m/sec)
air	340
water	1480
steel	5900
copper	4600
aluminum	6300
glass	5800
rubber	1040
silica sand[a]	243
50/80 silica sand[b]	212-454

a. Reported by Brown et al. (2007)
b. Reported by Charlie et al. (1990)

Table 2
Quikrete #1961 Properties

[a]USCS Classification	SP
Specific Gravity	2.72
D_{10} Partical Size (mm)	0.137
D_{30} Partical Size (mm)	0.211
D_{50} Partical Size (mm)	0.281
D_{60} Partical Size (mm)	0.320
[b]C_u	2.33
[c]C_c	1.02
[d]Percent Passing #100 sieve (%)	12.5
[d]Percent Passing #200 sieve (%)	2.7
[e]Maximum Dry Density (kg/m^3)	1630
[e]Minimum Dry Density (kg/m^3)	1400

Notes:
a. Unified Soil Classification System
b. Coefficient of Uniformity
c. Coefficient of Curvature
d. ASTM D4253
e. ASTM D4254

Table 3

Percent Volume of air for a given moisture content

% Moisture	Wet Density	% Saturation	% Vol. of Air
3%	1.55 g/cc	11%	38.5
4%	1.56 g/cc	14%	37.0
5%	1.58 g/cc	18%	35.5
7%	1.61g/cc	25%	32.5
9%	1.64 g/cc	32%	29.5
11%	1.67 g/cc	39%	26.4
13%	1.70 g/cc	46%	23.4
20%	1.80 g/cc	70%	13.0